Hydrol. Earth Syst. Sci. Discuss., 11, 4879–4924, 2014
www.hydrol-earth-syst-sci-discuss.net/11/4879/2014/
doi:10.5194/hessd-11-4879-2014

Hydrology and Earth System Sciences
Open Access
Discussions

Tracer-based analysis of spatial and temporal variation of water sources in a glacierized catchment

D. Penna[1,2,3], M. Engel[2,4], L. Mao[5], A. Dell'Agnese[2], G. Bertoldi[4], and F. Comiti[2]

[1]Department of Environment Sciences System, Swiss Federal University of Technology (ETH), Universitätstrasse 16, 8092 Zurich, Switzerland
[2]Faculty of Science and Technology, Free University of Bozen-Bolzano, piazza Università 5, 39100 Bolzano, Italy
[3]Department of Land, Environments, Agriculture and Forestry, University of Padova, viale dell'Università 16, 35020 Legnaro (PD), Italy
[4]Institute for Alpine Environment, EURAC, viale Druso 1, Bozen-Bolzano, Italy
[5]Department of Ecosystems and Environment, Pontificia Universidad Católica de Chile, Av. Vicuña Mackenna 4860, Macul, Casilla 306–22, Santiago, Chile

Received: 17 April 2014 – Accepted: 3 May 2014 – Published: 15 May 2014

Correspondence to: D. Penna (dpenna@ethz.ch)

Published by Copernicus Publications on behalf of the European Geosciences Union.

Abstract

Snow-dominated and glacierized catchments are important sources of fresh water for biological communities and for population living in mountain valleys. Gaining a better understanding of the runoff origin and of the hydrological interactions between meltwater and streamflow is critical for natural risk assessment and mitigation as well as for effective water resources management in mountain regions. This study is based on the use of stable isotopes of water and electrical conductivity as tracers to identify the water sources for runoff and their seasonal variability in a glacierized catchment in the Italian Alps. Samples were collected from rainfall, snow, snowmelt, ice melt and stream water (from the main stream at different locations and from selected tributaries) in 2011, 2012 and 2013. The tracer-based mixing analysis revealed that, overall, snowmelt and glacier melt were the most important end-members for stream runoff during late spring, summer and early fall. The temporal variability of the tracer concentration suggested that stream water was dominated by snowmelt at the beginning of the melting season (May–June), by a mixture of snowmelt and glacier melt during mid-summer (July–early August), and by glacier melt during the end of the summer (end of August–September). The same seasonal pattern observed in streamflow was also evident for groundwater, with the highest electrical conductivity and least negative isotopic values found during periods of limited melting. Particularly, the application of a two-component mixing model to data from different springs showed that the overall snowmelt contribution to groundwater recharge during the three study years ranged between 58 % (±15 %) and 72 % (±15 %). These results provided new insights on the isotopic characterization of the study catchment and the presented approach could offer further understanding of the spatio-temporal variability of the main water sources contributing to runoff in other snow-dominated and glacierized Alpine catchments.

HESSD
11, 4879–4924, 2014

1 Introduction

High-elevation mountain catchments are environments of highly economic and social value since they store large volumes of water in form of snow and glacier bodies and release it on a seasonal basis as meltwater. Large populations living downstream of glacierized catchments primary rely on snow and glacier meltwater for drinking and irrigation needs (Kriegel et al., 2013). Meltwater plays also an important role in the aquatic ecology of downstream reaches, because it regulates summer stream temperatures, maintaining high-quality habitat for fish and cold-water communities (Grah and Beaulieu, 2013). From a hydrological perspective, snowmelt and glacier melt are important because moderate inter-annual variability in streamflow (Stewart, 2009) and can maintain elevated discharge during the dry season or relatively dry years (Milner et al., 2009) when water demand is highest.

High-elevation catchments are complex environmental systems where different water sources interact to affect the streamflow regime and the geochemical composition of stream water. Understanding such a complexity is a first step toward a better conceptualization of catchment functioning that is critical for natural risk assessment and mitigation as well as for effective water resources management in mountain regions. This is even more critical under the current changing climatic conditions, to which snow-dominated and glacierized environments are particularly vulnerable. Thus, the expected future retreat of mountain glaciers and earlier melt of snowpack is producing marked effects on the water balance. In future, mean annual runoff is expected to decrease but peak runoff is likely to increase (Molini et al., 2011), with seasonal shifts in the runoff regime (Kääb et al., 2007) and in the relative timing and contribution of the different water sources on baseflow, peak flow and groundwater. This raises major concerns about water supply security in mountain regions (Uhlmann et al., 2013).

In this context, there is an urgent need to obtain a more detailed understanding of hydrological processes and of runoff origin in glacierized catchments, in order to better predict the future hydrological behaviour in such rapidly changing environments.

HESSD
11, 4879–4924, 2014

This would allow developing a broader view encompassing the dynamic interactions between meltwater and streamflow to eventually conceptualize the catchment internal hydrological functioning. For this purpose, a powerful investigation tool is represented by tracers. Particularly, the stable isotopes of water (δ^2H and δ^{18}O) have been recently used in high-elevation catchments to quantify post-snowmelt summer rainfall contributions to streamflow (Dahlke et al., 2013), estimate the regional water balance (Ohlanders et al., 2013), compute catchment residence times (Jeelani et al., 2013; Chiogna et al., 2014) and constrain model parameters (Cable et al., 2011). Moreover, water isotopes, coupled to other geochemical tracers, such as electrical conductivity (EC), have the potential to identify end-members (i.e., the dominant sources to runoff) and compute their contribution to streamflow (Maurya et al., 2011).

The discharge due to snow and glacier meltwater during spring and summer is relevant for the yearly runoff regime of streams in high-elevation Alpine areas (Koboltschnig and Schöner, 2011). Particularly, inner valleys of the Alps are characterized by relatively low amounts of liquid precipitation and significantly benefit from the water contribution provided by lateral valleys where snowmelt and/or glacier melt dominate streamflow. One clear example is given by the Vinschgau/Venosta valley, in South Tyrol (Eastern Italian Alps). The primary voice in the economy of population living there is the cultivation of apples. Since the climate is relatively dry (the mean annual precipitation for the period 1989–2012 in Laas-Lasa, at 863 m a.s.l., was 480 mm) a large part of water supply derives from stream water from the tributaries of the main valley, which are used for pressurized irrigation and hydropower production. Given the socio-economic importance of meltwater in this region, we conducted an experimental research in the glacierized Saldur catchment, one of the catchments that contribute to water availability in the Vinschgau valley. Importantly, the glacier in the Saldur catchment is melting at a particularly fast rate, with 20 % of areal reduction from 2005 to 2013 (Galos and Kaser, 2014). The Saldur catchment has been recently objective of different hydrological studies (e.g., Bertoldi et al., 2014; Della Chiesa et al., 2014; Pasolli et al., 2014)

HESSD
11, 4879–4924, 2014

but an assessment of the runoff water sources and of their spatio-temporal variability along with an isotopic characterization of the catchment is still missing.

In this paper, we take advantage of the combined use of two tracers, namely stable isotopes of water and EC, sampled from precipitation and different water bodies of three consecutive years, to:

1. define the origin of vapour masses that form precipitation in the study area;
2. identify the end-members to streamflow;
3. understand the seasonal variability of snowmelt and ice melt contribution to runoff;
4. quantify the role of snowmelt on groundwater recharge.

2 Study area

The field activities were carried out in the upper Saldur/Saldura catchment (61.7 km^2) lying in the upper Vinschgau/Venosta valley, South Tyrol (Eastern Italian Alps). Elevations in the catchment range from 1632 m a.s.l. at the outlet – chosen at a gauging station upstream of the confluence with the Etsch/Adige River – to 3725 m a.s.l. of the highest peak (Weißkugel/Palla Bianca). The upper part of the catchment hosts the Matsch/Mazia glacier (extent of 2.2 km^2 in 2013, Galos and Kaser, 2014) whose current snout lies approximately at 2800 m a.s.l. and feeds the Saldur River. Downstream of the glacier snout, the Saldur River receives water contributions from various tributaries, most of them, especially on the left side of the valley, originated at elevations above 2900 m a.s.l. and therefore seasonally covered by snow. As such, streamflow during summer and part of spring and fall is noticeably affected by water inputs mainly deriving from melting of the glacier body and of the winter snowpack in different portions of the catchment. Glacier erosion formed the typical U-shape in the upper valley that is partly filled with sediment from talus, small shallow landslides and large alluvial/debris

HESSD
11, 4879–4924, 2014

fans from the steep tributaries. The average slope of the catchment is 31.8° and the aspect is predominantly towards south (Table 1).

The study area has a continental climate with low total annual precipitation compared to other mountain areas at the same elevation. At 1570 m a.s.l., the mean annual air temperature is 6.6 °C and the mean annual precipitation is 569 mm, which increases up to 800–1000 mm at 2000 m a.s.l.. Precipitation typically occurs as snowfall from November to late April, while summer precipitation mainly originates from convective rainfall events. However, snow storms can occur also during the summer at the higher elevations.

Snow cover is almost complete at least over the upper three quarters of the Saldur catchment until late April–early May, when the melting season begins. Typically, at the end of June–early July snow cover amounts to approximately 10 % of the total catchment area, as revealed by snow surveys and snow cover estimations based on MODIS data (Notarnicola et al., 2013). Permafrost and rock glaciers are present at elevations higher than 2600–2800 m a.s.l., depending on local conditions (Boeckli et al., 2012, see Table 1). The Saldur River has a nivo-glacial regime, with minima recorded during the winter and maxima typically observed in late spring-early summer. The average winter discharge at the catchment outlet during the 2012–2013 winter period was around 0.38 $m^3 s^{-1}$ whereas during summer 2013 was 3.99 $m^3 s^{-1}$. The highest discharge since the start of monitoring (May 2009) was measured during a melt event on 21 June 2013 and reached 25.9 $m^3 s^{-1}$, whereas the second highest peak was recorded during a rain-on-snow event on 4 September 2011 and reached 18.2 $m^3 s^{-1}$.

Geologically, the Saldur basin belongs to the Matsch Unit, located in the southern Ötztal-Stubai complex. The base of the Matsch Unit belongs to the Vinschgau Shear Zone, that changes in the Schlinig fault. The Matsch Unit mainly consists of gneisses, mica gneisses and schists. The land cover within the catchment is dominated by bare rocks and bare soil (47 %), grassland (38 %) and forest (10 %) (CORINE90). The main grass vegetation *Nardion strictae* represents mostly the vegetation type at the bottom of the upper valley while the shrub vegetation *Rhododendro-Vaccinion* covers mostly

HESSD
11, 4879–4924, 2014

the valley slope. Haplic Leptosol are present above the tree line (at 2300 m a.s.l.), while forest, especially the north-facing slopes are mainly characterized by Haplic Podsols. Managed meadows below 1800 m a.s.l. are mostly characterized by Distric Cambisols. Soil texture can be classified between loamy sand and sandy loam (Bertoldi et al., 2014).

The upper catchment is weakly affected by human pressures. The uppermost permanently-lived building is at 1824 m a.s.l. and a small and steep gravel road goes up to around 2220 m a.s.l.. Only below 1800 m a.s.l. irrigated and intensively managed meadows are present. A limited net of tracks, mainly hiked during July and August, crosses the middle and upper part of the catchment. Cattle graze in the area at elevations up to 2400 m a.s.l. but sheep and goats can be found at much higher elevations.

3 Materials and methods

Hydrometeorological data used in this study were collected in the middle and upper part of the Saldur catchment approximately from April 2011 to October 2013. Precipitation and temperature were measured every 15 min by two non-heated weather stations (Onset Corporation, USA), labelled M3 and M4 (Fig. 1) at 2332 and 1998 m a.s.l., respectively and managed by the Institute for Alpine Environment of EURAC. For data analysis, the average values from these stations were used. Winter precipitation in these stations was validated using precipitation data and automatic recorded snow height data from nearby stations of the EURAC network by using the approach suggested by Mair et al. (2013).

Water stage was measured every ten minutes by pressure transducers at the catchment outlet (1632 m a.s.l.) by the Hydrographic Office of the Province of Bozen-Bolzano, and at two cross sections on the main channel, named Lower Stream Gauge (S3-LSG, 2150 m a.s.l.) and Upper Stream Gauge (S5-USG, 2340 m a.s.l.). The drainage area of these two sub-catchments is 18.6 and 11.2 km^2, respectively (Table 1). Water stage was converted to discharge by means of 82 salt dilution discharge

HESSD
11, 4879–4924, 2014

measurements taken under different flow conditions, in a range of 0.58 to 4.5 $m^3 s^{-1}$. Water stage was also measured on a tributary on the left side of the valley (T2-SG, 2027 m a.s.l., drainage area of 1.7 km^2) but direct discharge measurements were not available to build a reliable flow rating curve.

Stable isotopes of water and EC were measured in rain water, stream water, groundwater, snow, snowmelt and ice melt. The majority of samples was collected between April and October of each monitoring year but occasional samples were also taken in winter, early spring and late fall, especially at the lowest sampling locations. Bulk precipitation was sampled at five locations at different elevations along a 1000 m gradient (Fig. 1 and Table 2) using a 5 L high-density plastic bottle with a 18.5 cm diameter funnel. A mosquito net was placed inside the funnel to prevent leaves, particles or insects falling into the sampler. Bottles were filled with 1.5 cm of mineral oil to prevent evaporation and isotopic fractionation and replaced approximately every 45 days in 2011 and roughly monthly in 2012 and 2013. Stream water was sampled in the Saldur River at eight locations and in five tributaries between 1775 and 2415 m a.s.l. (Fig. 1 and Table 2). The tributaries were chosen to represent sub-catchments characterized by different hydro-geomorphological properties and size (Table 1).

Groundwater was sampled from four springs between 2334 and 2360 m a.s.l. on the right side of the valley (Fig. 1 and Table 2), named SPR1 to SPR4. SPR1 was located at the bottom of a hillslope. The water flow was relatively fast but stopped completely and the spring dried out in October 2011 and 2013. SPR2 was surrounded by rocks in a ponding area and the flow was very slow. SPR3 was located close to the stream and connected to it (water flowing from the spring evidently moved downslope towards the stream). Similarly, SPR4 was characterized by evident bubbling from sand sediment and flowing down to the stream. Samples of stream water and groundwater were collected approximately monthly.

The snowpack was sampled by snow corers. Three snow pits were dug on 8 March 2012 (at 1998, 2185, and 2205 m a.s.l.) and two on 6 February 2013 (at 1998 and 2085 m a.s.l.) and snow samples were taken at different layers. Moreover, three

HESSD
11, 4879–4924, 2014

samples of fresh snow were collected in the lower part of the catchment after two snowfalls in spring 2012. A few other snow cores were taken occasionally, in spring and summer, at other locations and higher elevations. Snowmelt was sampled by collecting water dripping from snow patches, residual of the winter snowpack, approximately between 2190 and 2815 m a.s.l.. Furthermore, the integrated value of snowmelt during the spring was measured using plastic snowmelt lysimeters (Shanley et al., 2002), with an approximate collecting area of 1 m^2, connected to a 20 L close bucket by 1 m long plastic tube. A 2 cm layer of mineral oil was put in the bucket during the lysimeter installation to prevent evaporation. Two lysimeters were placed at S3-LSG and one at 2205 m a.s.l. in fall 2011 and two at 2205 and 2225 m a.s.l. in fall 2013. They were emptied in mid-May 2012 and at the beginning of June 2013, respectively. Ice melt was collected by sampling rivulets flowing on the surface of the glacier tongue, approximately at 2800 m a.s.l.. Additionally, some samples of water slowly dripping from melting debris-covered ice (part of a disconnected glacier mass) were taken near the glacier snout. Throughout the paper, we refer to glacier melt and debris-covered ice melt to distinguish between the two types of ice melt sampling methods. Snowmelt and ice melt samples were taken occasionally during the summer and early fall of the three monitoring years. Overall, 598 water samples were taken during the observational periods. The position of all field instruments and rainfall, stream water and groundwater sampling locations is displayed in Fig. 1.

All water samples were collected in 50 mL high-density plastic bottles with a double cap, leaving no headspace. The samples were stored in the dark at 4 °C before isotopic analysis. The isotopic composition of the water samples was determined at the Laboratory of Isotope and Forest Hydrology of the University of Padova (Italy), Dept. of Land, Environments, Agriculture and Forestry by an off-axis integrated cavity output spectroscope (model DLT-100 908–0008, Los Gatos Research Inc., USA, see Penna et al., 2010, 2012). The typical instrumental precision (average standard deviation of 2094 samples) is 0.5 ‰ for δ^2H and 0.08 ‰ for δ^{18}O. EC was measured in the field using a portable conductivity meter with a precision of ±1 µS cm^{-1}.

HESSD
11, 4879–4924, 2014

Starting from δ^2H and δ^{18}O data, we computed the deuterium-excess (d-excess) for each sample, defined as (Dansgaard, 1964):

$$\text{d-excess} = \delta^2\text{H} - 8\delta^{18}\text{O} + 10. \quad (1)$$

Low d-excess values indicate that evaporation fractionation has occurred, and this leads to a change in the slope of the relationship between δ^{18}O and δ^2H. The d-excess represents the intercept of the linear fit line between δ^{18}O and δ^2H data in precipitation at the global scale, named global meteorological water line (GMWL, Craig, 1961) and defined as:

$$\delta^2\text{H}(‰) = 8\delta^{18}\text{O} + 10. \quad (2)$$

The d-excess in precipitation is related to humidity and temperature at the moisture source (Dansgaard, 1964) and therefore is useful to infer the origin of water vapour that determines precipitation in the study area (Cui et al., 2009; Wassenaar et al., 2011; Hughes and Crawford, 2013). In South-Western Europe, precipitation data that show d-excess close to the one of the GMWL typically indicate an Atlantic origin of air masses whereas higher d-excess may reflect the influence of water vapour coming from the Mediterranean basin, for which the local Mediterranean meteoric water line (MMWL) is valid (Gat and Carmi, 1970):

$$\delta^2\text{H}(‰) = 8\delta^{18}\text{O} + 22. \quad (3)$$

The computation of the snowmelt contribution to groundwater recharge was performed by using a simple two-component separation model (Pearce et al., 1986), based on water and tracer mass balance, as follows:

$$Q_1 = Q_2 + Q_3 \quad (4)$$

$$Q_1C_1 = Q_2C_2 + Q_3C_3 \quad (5)$$

$$Q_2 = [(C_1 - C_3)/[(C_2 - C_3)] \times Q_1 \quad (6)$$

HESSD
11, 4879–4924, 2014

where Q_1, Q_2 and Q_3 represent three different water components and C_1, C_2 and C_3 represent their tracer concentrations. On the basis of Eq. (6), we quantified the percentage of snowmelt contribution to groundwater recharge (SNML %) using d^2H data, as follows (Earman et al., 2006; Zhang et al., 2009):

$$\text{SNMLT\%} = [(C_{\text{SPR}} - C_{\text{RF}})/(C_{\text{SNM}} - C_{\text{RF}})] \times 100 \quad (7)$$

where C_{SPR} is the average isotopic composition of all samples collected from each spring over the three monitoring periods, C_{RF} is the volume-weighted average isotopic composition of the 23 rainfall samples collected at the locations RF4 and RF5 (the ones closest and upstream the selected springs, Table 2 and Fig. 1) and C_{SNM} is the average isotopic composition of 16 snowmelt samples collected from melting snow patches at elevations higher than those of the springs. The 70 % uncertainty in the separation of the two components was estimated through the method suggested by Genereux (1998) that takes into account the difference between the isotopic composition of the components and the variability (expressed by the standard deviation) of the isotopic composition of each component. The smaller the difference and the larger the variability, the higher the uncertainty.

Given the covariance between δ^2H and $\delta^{18}O$ values of all samples, in the plots and analyses throughout the paper where information coming from both isotopes were redundant, we reported only results referring to δ^2H values.

4 Results and discussion

4.1 Tracer concentration in different waters

The different waters sampled in the Saldur catchment during this study showed a marked variability in tracer concentration (Fig. 2). Over the entire dataset, δ^2H values ranged from −26.1 to −202.0 ‰ and EC ranged from 1 to 461 $\mu S\,cm^{-1}$. Rainfall and winter snowpack samples were characterized by the most positive and the most

HESSD
11, 4879–4924, 2014

negative isotopic composition, with median values of −65. and −158.9 ‰ in δ^2H, respectively. Overall, snowmelt was intermediate between rainfall and snowpack (median δ^2H = −122.9 ‰) whereas ice melt was more enriched in heavy isotopes (median δ^2H = −101.3 ‰). Stream water from the main stream and the tributaries, and groundwater from the springs had similar isotopic composition (median δ^2H = −105.2, −103.4 and −104.7 ‰, respectively) but still statistically different (Kruskal–Wallis test significant at 0.05 level).

The median EC of rainfall (Fig. 2b) was 8 µS cm^{-1}, thus lower than the EC typically measured in precipitation both in urban catchments (e.g., Pellerin et al., 2008; Meriano et al., 2011) and in other mountain catchments in more natural settings (e.g. Lambs, 2000; Zabaleta and Antigüedad, 2013). Low EC in rainfall indicates low concentration of solutes and suggests a little or negligible influence of air masses coming from the Mediterranean Sea basin, rich in salts and therefore characterized by higher EC (see also Sect. 4.2). The median EC of snowmelt (from patches of old snow and from snowmelt samplers as a whole) and ice melt (glacier melt and debris-covered ice melt as a whole) was also low and very low, of 12 and 2 µS cm^{-1}, respectively. Thus, isotopes allowed to characterize the ice melt signature, compared to that of rainfall and snowmelt, more uniquely than EC. The median EC of stream water in the tributaries and groundwater was similar (232 and 222 µS cm^{-1}, respectively) and higher than that of the Saldur River (160 µS cm^{-1}) that clearly reflected the contribution of low EC snowmelt and ice melt (Sect. 4.7). EC samples of stream water and groundwater showed statistical differences even more marked than those shown by δ^2H data (Kruskal–Wallis test significant at 0.01 level). This reflects the fact that all expected water sources contributing to streamflow during rainfall events and melting periods (rainfall, snowmelt and ice melt) had low values of EC but contrasting isotopic composition that compensated when mixed in the Saldur River.

HESSD
11, 4879–4924, 2014

4.2 Isotopic composition of rainfall

The linear relationship between $\delta^{18}O$ and $\delta^{2}H$ composition of rainfall data collected at different elevations in the Saldur catchment defined a local meteorological water line (LMWL), expressed as (Fig. 3):

$$\delta^{2}H(‰) = 8.1\delta^{18}O + 10.3 \quad R^2 = 0.99, n = 66. \tag{8}$$

This relationship is slightly different from the LMWL of Northern Italy (Longinelli and Selmo, 2003; Longinelli and Stenni, 2008) defined as:

$$\delta^{2}H(‰) = 7.7\delta^{18}O + 9.4 \tag{9}$$

and also from the LWML found by Chiogna et al. (2014) for a station at 1176 m a.s.l. in a glacierized Alpine catchment between the Ortles-Cevedale and the Adamello–Presanella massifs (Northern Italy, approximately 44 km South in a straight line from the Saldur catchment), defined as:

$$\delta^{2}H(‰) = 7.6\delta^{18}O + 2.7. \tag{10}$$

Conversely, the LMWL in the Saldur catchment is quite similar to the one derived at the highest elevation reported by Chiogna et al. (2014) in similar climatic conditions, defined as:

$$\delta^{2}H(‰) = 8.0\delta^{18}O + 7.8. \tag{11}$$

It is evident that the slope of the Saldur LMWL (10.1) is higher than that of the other Northern Italian sites at lower elevations (7.7 and 7.6, Eqs. 9 and 10, respectively), but approximately the same to that in a mountain region at higher elevation (8.0, Eq. 11). More interestingly, both the slope and the d-excess of the Saldur LMWL are nearly identical to those of the GMWL (Eq. 2) and d-excess is noticeably different from that of the MMWL (Eq. 3). Although a full comparison among these relationships cannot be

HESSD
11, 4879–4924, 2014

made because the LMWL at our site did not include samples collected during the winter, this reveals that precipitation (at least during late spring, summer and early fall) in the Saldur area, and likely in other left-side lateral valleys of the Upper Vinschgau valley, was predominantly originated by air masses developing on the Atlantic Ocean, with limited influence by inflow of water vapour from the Mediterranean sea. This confirms what indicated by the very low EC observed in rainfall (Sect. 4.1).

Figure 3 also highlights the clear and expected temperature-dependent seasonality (e.g. Wassenaar et al., 2011) with heavier isotopic values occurring during the summer, lighter values occurring during the fall and intermediate values generally occurring during the spring, and partially overlapping with the most negative summer samples and the most positive fall samples. In addition, the inset reported in Fig. 3 displays the variation of average δ^2H of rainfall samples ($n = 8$) as a function of the station elevation, revealing a marked altitude effect (Araguás-Araguás et al., 2000), recognized in almost all mountain ranges worldwide (Poage and Chamberlain, 2001). Particularly, the linear relationship between the average isotopic composition of rainfall samples and elevation in the Saldur catchment yielded an isotopic depletion rate of −1.6 ‰ for δ^2H and −0.23 ‰ for δ^{18}O per 100 m rise in elevation. This gradient is steeper than that found in a snowmelt- and glacier melt-dominated Andean catchment, Chile (Ohlanders et al., 2013), and by Chiogna et al. (2014), and is gentler than that in the Kumaon Himalayas, India (Kumar et al., 2010). However, the gradient is fully consistent with that in Kashmir Himalaya (Jeelani et al., 2013) and with the one reported by Longinelli et al. (2006) for an Alpine region in North-Western Italy.

Elevation played also a role on the spatial variability of d-excess in precipitation. Although the relationship was less strong than the one between elevation and δ^2H and δ^{18}O in rainfall, our data (not reported) showed that d-excess (the average of data available for all five sampling locations, $n = 8$) increased roughly linearly of 0.2 ‰ per 100 m rise in elevation ($R^2 = 0.69$, $n = 5$, significant at 0.1 level). This effect was also reported for other mountain areas (Cui et al., 2009; Kumar et al., 2010; Jeelani et al., 2013). In some cases, the increase of d-excess with altitude was reported to be mainly

HESSD
11, 4879–4924, 2014

present at high relative humidity (Gonfiantini et al., 2001; Windhorst et al., 2013) which is not the case of the study area. In the Saldur catchment, this effect may be attributed to higher relative humidity at higher elevations due to snow and ice melting which tends to enhance the kinetic fractionation process during evaporation (cf. Peng et al., 2004). However, additional unknown factors (Gat et al., 2000) might be claimed to explain the observed altitude effect of d-excess.

4.3 Isotopic composition of snow, snowmelt and ice melt

Snow samples taken from the winter snowpack covered a broad isotopic range, spanning from −134.9 to −202.0 ‰ in δ^2H and from −18.34 to −26.46 ‰ in δ^{18}O (Fig. 4), reflecting a wide variability in air temperature that may have occurred also during the winter. Moreover, snow samples fell well on the LMWL (and therefore on the GMWL), as also confirmed by the slope and interception values very similar to those of the LMWL (Table 3). This indicates a similar geographical origin of precipitation during the winter with respect to the other seasons. Samples collected from melting snow patches showed a wide isotopic range too, varying from −106.1 to −165.4 ‰ in δ^2H and from −14.26 to −21.47 ‰ in δ^{18}O (Fig. 4). This likely reflects the different elevations where the samples were collected and, at the same time, the progressive seasonal isotopic enrichment that snowpack underwent during the melting process (Taylor et al., 2001; Lee et al., 2010). Meltwater samples of snow patches laid on the LMWL too (Fig. 4), and were characterized by values of slope and intercept very similar to those of the LMWL (Table 3), indicating no or negligible secondary fractionation effects due to evaporation during deposition and melting processes. Winter- and spring-integrated snowmelt samples taken from the lysimeters also followed the LMWL but were slightly below it (Fig. 4) and showed slightly smaller slope and intercept (Table 3). Moreover, except for three samples, snowmelt samples collected from lysimeters were isotopically heavier than snowmelt samples collected from snow patches. This difference was related to some possible contamination from relatively less negative precipitation during the spring. The three samples with more negative values were collected in spring 2012

HESSD
11, 4879–4924, 2014

from snow lysimeters localized close to the stream at S3-LSG, in a zone where the valley is relatively narrow and direct sunlight is limited.

Ice melt samples generally plotted on the LMWL but, in accordance to Gooseff et al. (2006), the slopes and the intercepts of their δ^{18}O-δ^{2}H relationships for both glacier melt and debris-covered ice melt were slightly smaller than those of the LMWL (Table 3). A comparison of the isotopic composition of glacier meltwater in the Saldur catchment with samples taken in other parts of the globe reveals the variability of dominant climatic conditions. Saldur glacier melt was more depleted compared to the Mafengu River, China (Yang et al., 2012), similar to the Ganga River catchment in the Himalayan foothills (Maurya et al., 2011) and in the Langtang and Dudh Kosi basins in Nepal Himalaya (Racoviteanu et al., 2013). However, it was heavier than that in the Wind River Range in the American Rockies (Cable et al., 2001) and a Central Andean catchment (Ohlanders et al., 2013) and, not surprisingly, much heavier than that found at the Imersuaq Glacier, West Greenland (Yde and Knudsen, 2004).

The isotopic range of glacier melt and debris-covered ice melt samples collected in the Saldur catchment was similar (Fig. 4), with average δ^{2}H = −102.3 ‰ and standard deviation = 7.8 ‰ for glacier melt (n = 16), and average δ^{2}H = −100.2 ‰ and standard deviation = 4.9 ‰ for debris-covered ice melt (n = 9). However, glacier melt typically showed higher d-excess (12.7 ‰ vs. 11.0 ‰) but similar variability of d-excess (standard deviation of 1.2 ‰ vs. 1.4 ‰) compared to debris-covered ice melt. This difference was likely associated to the aforementioned increase in d-excess with elevation (Sect. 4.2), since the rivulets sampled on the glacier surface originated at higher elevations compared to the debris-covered ice collected nearby the glacier snout. Moreover, the expected lower melt rate due to the debris coverage, compared to the melt occurring on the bare glacier surface, might have also determined secondary evaporation effects (confirmed by the slightly smaller slope compared to glacier melt, Table 3) contributing to the difference in d-excess between the two subsets. However, the most striking difference between the two types of ice melt samples lays in the much higher and more variable EC of meltwater derived from ice bodies covered

HESSD
11, 4879–4924, 2014

by debris (average = 66 µS cm^{-1}, standard deviation = 40 µS cm^{-1}, n = 6) compared to the extremely low (almost distilled) and little variable EC of glacier meltwater (average = 2 µS cm^{-1}, standard deviation = 0.7 µS cm^{-1}, n = 16). This difference, reflecting the very high variability in EC of all ice melt samples (glacier melt and debris-covered ice melt, Fig. 2b), was not unexpected considering the contact that the latter had with rocks and fine debris that could release salts increasing the EC of meltwater.

4.4 Isotopic composition of stream water and groundwater

The isotopic composition of stream water showed a narrower range compared to rainfall, snowmelt and ice melt (Fig. 2a) indicating that waters originating from upstream sources mixed to give composite stream water (Dalai et al., 2002; Maurya et al., 2011). The slope of 7.9 of the δ^{18}O-δ^{2}H relationship of stream water in the Saldur River (Table 4) was similar to that of rainfall (Fig. 3) and especially to that of snowmelt (Table 3), reflecting well the isotopic signal of this water source. On the contrary, groundwater and stream water in the tributaries showed lower slopes of the δ^{18}O-δ^{2}H relationship compared to the Saldur River waters and to rainfall samples (and therefore a departure from the LMWL, not shown) suggesting post-precipitation evaporation during the groundwater recharge process (Maurya et al., 2011), as discussed in Sect. 4.9.

4.5 Identification of end-members

The average values of δ^{2}H plotted vs. d-excess for all stream water and groundwater samples fell within a triangular domain defined by the average δ^{2}H and d-excess (Machavaram et al., 2006) of rainfall, snowmelt and glacier melt (Fig. 5). Unfortunately, since we were able to measure rainfall intensity but not snowmelt and glacier melt intensity, only the δ^{2}H and d-excess values of rainwater samples were volume-weighted whereas snowmelt and glacier melt were not. This could affect mass balance computations but it is reasonable to assume that this would not change the general evidence provided by Fig. 5. Indeed, despite the large variability of measurements in all

HESSD
11, 4879–4924, 2014

waters (long error bars), the mixing plot clearly reveals the importance of snowmelt and glacier melt as end-members in the study catchment, playing therefore a major role on the runoff regimes of the Saldur River and of its tributaries, as also observed in other glacierized catchments (Zhang et al., 2009; Dahlke et al., 2013; Olhanders et al., 2013). However, it must be mentioned that we normally collected samples during no-rain periods, and therefore the contribution of rain water to the isotopic and EC composition of stream water and groundwater was likely underestimated. Although the error bars of samples within the triangular space largely overlapped, it is interesting to note that samples taken in the main stream were closer to the glacier melt end-member than the samples collected in the tributaries, and that the samples collected from the springs fell closer to the snowmelt end-member than stream water samples. This indicates, as expected, that glacier melt was a more important contributor to runoff in the main stream, distinctly glacier-fed, compared to the tributaries, and suggests an important role of snowmelt on groundwater recharge (Sect. 4.9). Snowpack samples were not included in the mixing plot simply because winter snowpack cannot be considered as a direct hydrological input.

4.6 Temporal hydrological dynamics

The three observational periods considered in this study showed different hydrometeorological characteristics (Fig. 6). The average temperature over the 1 April–31 October period was similar for the three years (6.7, 6.5 and 6.3 °C for 2011, 2012 and 2013, respectively) but the temporal variability slightly differed. Most of all, cumulative precipitation was noticeably different, with 536, 467 and only 380 mm over the same period in 2011, 2012 and 2013, respectively. However, although 2013 was the driest year, streamflow and water stage at the gauging stations, especially at S5-USG, showed marked responses, suggesting important contributions of meltwater. At the end of April-beginning of May, when the melting season started, streamflow in the main stream (Fig. 6g–l) and water stage in the tributary T2-SG (Fig. 6m–o) were typically low with values close to the winter baseflow (below 0.5 $m^3 s^{-1}$ at S5-USG,

HESSD
11, 4879–4924, 2014

1 $m^3 s^{-1}$ at S3-LSG and 5 cm at T2-SG). Then, streamflow noticeably increased during the warmer months (June–August) up to 3–4 $m^3 s^{-1}$ at S5-USG, 6–7 $m^3 s^{-1}$ at S3-LSG and 25–30 cm at T2-SG, and started to recede in September, reflecting the combination of limited snow cover and incoming radiation too small to produce important melt. Additionally, streamflow showed a marked diurnal variability (Josh et al., 2012; Uhlmann et al., 2013), particularly in the main stream and slightly less evident in the tributary, with clear fluctuations dependent on daily temperature oscillations that triggered the release of meltwater to the stream network (Fig. 6d–o).

At the seasonal scale, the melting dynamics seemed to override the role of rainfall on streamflow variability. Typical rainfall events were characterized by daily cumulative amounts less than 10 mm that produced small streamflow response and limited sediment transport (Mao et al., 2014). However, the highest streamflow peaks were associated to relatively intense rainfall events. For example, 19.6 mm of rain fell in four hours on 4 September 2011 and produced streamflow hourly peaks of 5.3 $m^3 s^{-1}$ at S5-USG, 8.0 $m^3 s^{-1}$ at S3-LSG and water stage peak of 37 cm at T2-SG, observed almost simultaneously at all three gauging locations.

4.7 Spatio-temporal dynamics of tracer concentration in stream water and groundwater

4.7.1 Temporal variability of stream water and groundwater EC and δ^2H

The isotopic composition of stream water (Fig. 6g–o) did not reflect the seasonal variation of isotopes in rainfall, with the less negative values occurring during the warmest periods (Sect. 4.2) but tended to mirror it (Jeelani et al., 2013). Indeed, the samples collected in the Saldur River and its selected tributaries revealed that during the late spring and the beginning of the summer (June–July) δ^2H in stream water was relatively depleted in heavy isotopes (ranging approximately between −115 and −110 ‰), then increased during mid-late summer up to values close to the baseflow background (Fig. 6). Similarly, EC was relatively high before the beginning of the melting period (up

HESSD
11, 4879–4924, 2014

to approximately 250 µS cm^{-1} at S3-LSG), then decreased below 100 µS cm^{-1} during the melting season and increased to background values in mid-late October (Fig. 6). This pattern was less clear in 2011 in the main stream (Fig. 6g and j) because samples were collected at different times of the day and therefore the variability in tracer composition, due to the daily streamflow fluctuations induced by meltwater inflows, masked the seasonal evolution. However, given the very low EC and the significantly more negative values of snowmelt and ice melt compared to rainfall (Fig. 2), the general pattern suggests a remarkable (even though not easily quantifiable) contribution of meltwater to runoff in the Saldur catchment, confirming the results of the end-member mixing analysis (see Fig. 5 and Sect. 4.7.3).

This trend was also revealed by the δ^2H and EC of four locations along the Saldur River, for which we collected samples approximately monthly during all three monitoring years, of three tributaries for which we have the most numerous data and of the four selected springs (Fig. 7). The overall pattern of more negative isotopes and relatively low EC at the beginning and at the peak of the melting season was evident. Analogously, less negative isotopes and higher EC were observed at the end of the season. Overall, this pattern was temporally consistent for stream water, both in the main stream and in the tributaries, and for groundwater. The increasing trend in isotopic composition and EC of the springs and the tributaries (generally with a negligible glacierized area compared to that of the main stream sub-catchments, see Table 1) likely reflects the decreasing contribution of snowmelt over the season. Moreover, the relatively fast dynamics of tracer concentrations in the springs suggested low residence times in the catchment (Jeelani et al., 2010). Isotopes in the Saldur River in August 2013 (Fig. 7a) were noticeably less negative compared to the previous sampling and disagreed with the isotopic composition of the springs (Fig. 7c) that continued the negative trend before increasing on the last sampling date. One reason for this difference could be related to the lagged arrival of the snowmelt contribution to the springs but this should be verified by means of additional data and possibly modelling application.

HESSD
11, 4879–4924, 2014

4.7.2 Spatial variability of stream water and groundwater EC and δ^2H

The consistency of temporal patterns over space, among the different locations, was particularly remarkable for the Saldur River locations and for springs SPR1-3 (Fig. 7a and c, respectively). Overall, location S8, higher in elevation and closer to the glacier snout (Table 2), showed the most extreme δ^2H and the lowest EC likely because it was more directly influenced by meltwater inputs. S3-LSG and S1, the locations more downstream, showed the highest EC, due to the comparatively higher contribution of groundwater. However, S3-LSG was characterised by relatively more negative δ^2H compared to S1 due to the inflow of the highly isotopically depleted tributary at location T4 (data not shown). SPR4 showed a clearly different isotopic composition and EC concentration and different patterns compared to the other three springs. So far, we do not have experimental data to explain these differences but a more detailed analysis of groundwater geochemical and microbiological composition at different locations in the Saldur catchment is in progress.

4.7.3 Seasonal change in snowmelt and ice melt contribution to runoff

Data of stream water tracer concentration collected in 2011, 2012 and 2013 at the same time of the day at four selected locations along the Saldur River (S1, S3-LSG, S5 and S8) were grouped according to the month of sampling and displayed as box-plots (Fig. 8). Stream water was relatively depleted in heavy isotopes in June, isotopically heavier and characterized by a large variability in July and slowly increasingly enriched in heavy isotopes in August, September and October (Fig. 8a). Interestingly, EC showed a different pattern, with low values and similar variability in June, July (slightly lower) and August and markedly higher distributions in September and October (Fig. 8a). Although this plot masks the inter-annual variability of tracer concentration and the number of samples is limited, the observation of the different dynamics of the two tracers gives some hints on the seasonal switch of the most important contributors to runoff of the Saldur River. Indeed, the negative δ^2H and low EC values found

HESSD
11, 4879–4924, 2014

in June might reflect a major contribution of snowmelt, depleted in heavy isotopes and with low EC (Fig. 2). The even lower EC but less negative and more variable isotopes in July might reflect a mixed contribution of snowmelt and glacier melt that had extremely low EC but less negative isotopic composition (Fig. 2). The still low EC but the relatively heavier isotopes in August might reflect a major contribution of glacier melt. Finally, the more enriched δ^2H and the higher EC in September and October suggest a little or negligible contribution of meltwater to the Saldur River, especially in October when the variability in the isotopic composition of stream water was very small.

The same conclusions can be drawn when looking at the spatio-temporal variability of tracer concentration at the same four selected locations along the main stream for different sampling days in 2013, the year where we have more data collected at approximately the same time of the day in different dates (Fig. 9). The low EC and the relatively heavier isotopes in stream water in August reflected particularly well the tracer composition of glacier melt, suggesting its dominant contribution to streamflow later in the melting season, when most of the catchment is typically snow-free. Moreover, the spatial pattern of tracer concentration along the stream was consistent among the different dates for EC (except for the decreasing value at S1 in October, Fig. 9b) and more gentle but still fairly similar for δ^2H. This general temporal persistence of spatial patterns of tracer concentration indicates that the contribution of different water sources and of tributaries to the stream was continuous over time (i.e., all water sources and all tributaries, although carrying a possibly different isotopic and EC signature, gave continuous contributions over time), also revealing a good water mixing in the stream.

4.8 Role of snowmelt on groundwater recharge

The application of the isotope-based two component separation model to spring water data (Eq. 7) allowed us to quantify the relative contribution of snowmelt to groundwater recharge, qualitatively assessed by the visual inspection of the temporal variability of tracer concentration in the selected springs (Sect. 4.7). Results revealed that, overall,

HESSD
11, 4879–4924, 2014

snowmelt played a relevant role on groundwater composition in the Saldur stream compared to rainfall, with contributions ranging from 58 % (±15 %) for SPR4 to 72 % (±15 %) for SPR2 (Table 5). Including ice melt data (both glacier and debris-covered ice melt) in the model gave inconsistent results, likely indicating the negligible contribution of ice melt to groundwater recharge. The very similar fractions among SPR1-3 and the different fractions compared to SPR4 agree, as expected, with the observed differences in the isotopic composition of the four springs (Fig. 7c and f). The comparatively minor role of summer precipitation in recharging groundwater is also confirmed by considering that the average isotopic composition of the springs was not consistent with the much more positive average isotopic composition of rainfall (Fig. 2a). When spring δ^2H was plotted on a rainfall δ^2H vs. elevation plot (not shown) to estimate the elevation of groundwater recharge (e.g., Jeelani et al., 2010) we obtained inconsistent results, i.e. the elevation of recharge was found to be much higher than the highest peak in the study area. This demonstrates the noticeably greater contribution of snow precipitation compared to liquid precipitation. This is probably not surprisingly considering the low precipitation amounts that characterize the study area during the summer. However, these results are important for the development of a perceptual model of the hydrological functioning of the Saldur catchment. Moreover, these results are in agreement with the upper limit of the isotopic-based estimates of the role of snowmelt on groundwater recharge in the South-Western US (Earman et al., 2006) and confirm previous observations from other high-elevation catchments (Earman et al., 2006; Jeelani et al., 2010, 2013).

5 Limitations of the research and concluding remarks

Spatially-distributed samples of rainfall, snowmelt, ice melt, groundwater and stream water were collected over three years in the glacierized Saldur catchment in the Eastern Italian Alps and analysed for stable isotopes of water and EC, allowing us to identify the main end-members and to explore the spatio-temporal variability of water sources.

HESSD
11, 4879–4924, 2014

Data collection in such a high-elevation and complex terrain proved to be particularly challenging, and some issues arose. For instance, sampling at higher temporal frequency might have allowed us to explore some short-time responses in tracer concentration and detect some finer dynamics (e.g., Neal et al., 2013). Moreover, samplings were not always taken at the same time of the day among the three years, preventing us to make comparisons on a more extended subset of data. More importantly, we were not able to sample permafrost (for instance, from rock glaciers) and winter precipitation beside snowpack (we experienced snowfall collectors failures for two consecutive winters), likely yielding an incomplete overview of all potential end-members in the study catchment. Analogously, as mentioned above, the lack of sampling during rain periods probably provided an underestimation of the role played by rain water on the isotopic and EC composition of stream water.

Despite these limitations, our study provided new insights on the isotopic characterization of waters in high-elevation Alpine basins, allowing us to take advantage of the enhanced tracer capability derived from the combined use of EC and water stable isotopes for identifying end-members. Particularly, from a methodological point of view, this research provided one of the largest isotopic database in glacierized catchments that we are aware of, even larger than some very robust datasets recently published (e.g. Ohlanders et al., 2013; Chiogna et al., 2014). Furthermore, our study was the first one, as far as we know, to provide samples of EC and isotopic composition of actual glacier melt in the Italian Alps, i.e. meltwater flowing directly on the glacier surface and not water discharging from the glacier snout (possibly mixed with groundwater inflows). This allowed a better characterization of the tracer concentration of this end-member. Finally, the observation periods that spanned three years across various seasons allowed us to identify temporally-invariant behaviours in tracer concentrations as well as to compare the inter-annual variability of water source dynamics, providing a broader idea of hydrological behaviours under different conditions.

HESSD
11, 4879–4924, 2014

6 Conclusions

In conclusions, the main results are the following:

- A marked variability in EC and isotopic composition of all sampled waters was evident, indicating a highly complex signature of water within the catchment. The combined signature provided by the two tracers yielded a clear distinction between input sources to the system, allowing us to identify snowmelt and glacier melt as the main end-members for stream water and groundwater, with a secondary role played by rainfall.

- Rainfall samples delineated a LMWL remarkably similar to the GMWL, suggesting a predominantly oceanic origin of air masses in the study area. In addition to the seasonal effect, a clear altitude effect was observed for rainfall samples, with an isotopic depletion rate of −1.6 ‰ for δ^2H and −0.23 ‰ for δ^{18}O per 100 m rise in elevation.

- Snow, snowmelt and ice melt samples fell along the LMWL, indicating little or negligible evaporation during the post-deposition processes. On the contrary, the isotopic composition of groundwater samples showed a post-precipitation evaporation effect.

- The temporal dynamics of tracer concentrations and, particularly, the different dynamics of EC with respect to δ^2H revealed a change in the main water source to the Saldur River runoff over the season, with snowmelt being the major contributor to streamflow during the first and central part of the melting period (June, July), whereas later in the summer, when most of the snow disappeared from the catchment, glacier melt contributed significantly. Despite such dynamics are well known in high-elevation catchments, their clear detection based on tracers is quite remarkable from a methodological perspective.

HESSD
11, 4879–4924, 2014

– The overall contribution of snowmelt to groundwater recharge, quantified by using an isotope-based two component separation model, ranged between 58 % (±15 %) and 72 % (±15 %), revealing the marked importance of snowmelt for subsurface water storage in the Saldur catchment.

Overall, these results shed new light on the main sources of water contributing to runoff and their spatio-temporal variability, information that were still missing in glacierized areas of South-Tyrol and are still very limited for the entire Southern Alps. These data provide preliminary and qualitative information on the temporal evolution of meltwater to the Saldur River network that will be compared with satellite images and modelling results. Moreover, in an ongoing work, two- and three-component hydrograph separation models, based on hourly tracer data, are being applied to selected runoff events in the study years (preliminary results in Penna et al., 2013). These analyses will permit quantitative estimates of the contribution of ice melt and snowmelt to stream water in different periods of the seasons and will lead to a better understanding of the role of meltwater dynamics on streamflow generation in high-elevation glacierized catchments of the Alps.

Acknowledgements. This work was financially supported by the research projects "Effects of climate change on high-altitude ecosystems: monitoring the Upper Match Valley" (Free University of Bozen-Bolzano) and "EMERGE: Retreating glaciers and emerging ecosystems in the Southern Alps" (Dr. Erich-Ritter- und Dr. Herzog-Sellenberg-Stiftung im Stifterverband für die Deutsche Wissenschaft). Support was also provided by the Dept. of Hydraulic Engineering and Hydrographic Office of the Autonomous Province of Bozen-Bolzano. The project "HydroAlp" financed by Autonomous Province of Bozen-Bolzano and partly supported the work of G. Bertoldi. G. Niedrist of EURAC is thanked for his work in maintaining the meteorological stations. Giulia Zuecco (University of Padova) is warmly thanked for the laser spectroscopy isotopic analysis. We thank Enrico Buzzi and Raffaele Foffa for support in field work. The first author is grateful to Ilja van Meerveld (VU University of Amsterdam) for discussions during a field trip, and to James W. Kirchner (ETH, Zurich) for discussions on the preliminary results.

HESSD
11, 4879–4924, 2014

References

Araguás-Araguás, L., Froehlich, K., and Rozanski, K.: Deuterium and oxygen-18 isotope composition of precipitation and atmospheric moisture, Hydrol. Process., 14, 1341–1355, doi:10.1002/1099-1085(20000615)14:8<1341::AID-HYP983>3.0.CO;2-Z, 2000.

Bertoldi, G., Della Chiesa, S., Notarnicola, C., Pasolli, L., Niedrist, G., and Tappeiner, U.: Estimation of soil moisture patterns in mountain grasslands by means of SAR RADARSAT 2 images and hydrological modelling, J. Hydrol., in review, 2014.

Boeckli, L., Brenning, A., Gruber, S., and Noetzli, J.: A statistical approach to modelling permafrost distribution in the European Alps or similar mountain ranges, The Cryosphere, 6, 125–140, doi:10.5194/tc-6-125-2012, 2012.

Cable, J., Ogle, K., and Williams, D.: Contribution of glacier meltwater to streamflow in the Wind River Range, Wyoming, inferred via a Bayesian mixing model applied to isotopic measurements, Hydrol. Process., 25, 2228–2236, doi:10.1002/hyp.7982, 2011.

Chiogna, G., Santoni, E., Camin, F., Tonon, A., Majone, B., Trenti, A., and Bellin, A.: Stable isotope characterization of the Vermigliana catchment, J. Hydrol., 509, 295–305, doi:10.1016/j.jhydrol.2013.11.052, 2014.

Craig, R.: Isotopic variations in meteoric waters, Science, 133, 1702–1703, 1961.

Cui, J., An, S., Wang, Z., Fang, C., Liu, Y., and Yang, H.: Using deuterium excess to determine the sources of high-altitude precipitation?: Implications in hydrological relations between sub-alpine forests and alpine meadows, J. Hydrol., 373, 24–33, doi:10.1016/j.jhydrol.2009.04.005, 2009.

Dahlke, H., Lyon, S., and Jansson, P.: Isotopic investigation of runoff generation in a glacierized catchment in northern Sweden, Hydrol. Process., 28, 1035–1050, doi:10.1002/hyp.9668, 2014.

Dalai, T. K., Bhattacharya, S. K., and Krishnaswami, S.: Stable isotopes in the source waters of the Yamuna and its tributaries: seasonal and altitudinal variations and relation to major cations, Hydrol. Process., 16, 3345–3364, doi:10.1002/hyp.1104, 2002.

Dansgaard, W.: Stable isotopes in precipitation, Tellus, 16, 436–468, 1964.

Della Chiesa, S., Bertoldi, G., Niedrist, G., Obojes, N., Endrizzi, S., Albertson, J. D., Wohlfahrt, G., Hörtnagl, L., and Tappeiner, U.: Modelling changes in grassland hydrological cycling along an elevational gradient in the Alps, Ecohydrology, doi:10.1002/eco.1471, in press, 2014.

HESSD
11, 4879–4924, 2014

Earman, S. and Campbell, A.: Isotopic exchange between snow and atmospheric water vapor: estimation of the snowmelt component of groundwater recharge in the southwestern United States, J. Geophys. Res., 111, 1–18, doi:10.1029/2005JD006470, 2006.
Froehlich, K., Kralik, M., Papesch, W., Rank, D., Scheifinger, H., and Stichler, W.: Deuterium excess in precipitation of Alpine regions – moisure recycling, Isot. Environ. Healt. S., 44, 61–70, 2008.
Galos, S. and Kaser, G.: The Mass Balance of Matscherferner 2012/13, project report, University of Innsbruck, Innsbruck, 2014.
Gat, J. R. and Carmi, I.: Evolution of the isotopic composition of atmospheric waters in the Mediterranean Sea area, J. Geophys. Res., 75, 3039–3048, 1970.
Genereux, D.: Quantifying uncertainty in tracer-based hydrograph separations, Water Resour. Res., 34, 915–919, doi:10.1029/98WR00010, 1998.
Gooseff, M. N., Lyons, W., McKnight, D. M., Vaughn, B. H., Fountain, A. G., and Dowling, C.: A stable isotopic investigation of a polar desert hydrologic system, McMurdo dry valleys, Antarctica, Arct. Antarct. Alp. Res., 38, 60–71, 2006.
Grah, O. and Beaulieu, J.: The effect of climate change on glacier ablation and baseflow support in the Nooksack River basin and implications on Pacific salmonid species protection and recovery, Climatic Change, 120, 657–670, doi:10.1007/s10584-013-0747-y, 2013.
Hughes, C. E. and Crawford, J.: Spatial and temporal variation in precipitation isotopes in the Sydney Basin, Australia, J. Hydrol., 489, 42–55, doi:10.1016/j.jhydrol.2013.02.036, 2013.
Jeelani, G., Bhat, N. A., and Shivanna, K.: Use of δ^{18}O tracer to identify stream and spring origins of a mountainous catchmen: a case study from Liddar watershed, Western Himalaya, India, J. Hydrol., 393, 257–264, doi:10.1016/j.jhydrol.2010.08.021, 2010.
Jeelani, G., Kumar, U. S., and Kumar, B.: Variation of δ^{18}O and δD in precipitation and stream waters across the Kashmir Himalaya (India) to distinguish and estimate the seasonal sources of stream flow, J. Hydrol., 481, 157–165, doi:10.1016/j.jhydrol.2012.12.035, 2013.
Jin, L., Siegel, D. I., Lautz, L. K., and Lu, Z.: Identifying streamflow sources during spring snowmelt using water chemistry and isotopic composition in semi-arid mountain streams, J. Hydrol., 470–471, 289–301, doi:10.1016/j.jhydrol.2012.09.009, 2012.
Jost, G., Moore, R. D., Menounos, B., and Wheate, R.: Quantifying the contribution of glacier runoff to streamflow in the upper Columbia River Basin, Canada, Hydrol. Earth Syst. Sci., 16, 849–860, doi:10.5194/hess-16-849-2012, 2012.

HESSD
11, 4879–4924, 2014

Kääb, A., Chiarle, M., Raup, B., and Schneider, C.: Climate change impacts on mountain glaciers and permafrost, Global Planet. Change, 56, vii–ix, doi:10.1016/j.gloplacha.2006.07.008, 2007.
Knoll, C.: A glacier inventory for South Tyrol, Italy, based on airborne laser-scanner data, Ann. Glaciol., 50, 46–52, 2010.
Koboltschnig, G. R. and Schöner, W.: The relevance of glacier melt in the water cycle of the Alps: the example of Austria, Hydrol. Earth Syst. Sci., 15, 2039–2048, doi:10.5194/hess-15-2039-2011, 2011.
Kriegel, D., Mayer, C., Hagg, W., Vorogushyn, S., Duethmann, D., Gafurov, A., and Farinotti, D.: Changes in glacierisation, climate and runoff in the second half of the 20th century in the Naryn basin, Central Asia, Global Planet. Change, 110, 51–61, doi:10.1016/j.gloplacha.2013.05.014, 2013.
Kumar, U. S., Kumar, B., Rai, S. P., and Sharma, S.: Stable isotope ratios in precipitation and their relationship with meteorological conditions in the Kumaon Himalayas, India, J. Hydrol., 391, 1–8, doi:10.1016/j.jhydrol.2010.06.019, 2010.
Lambs, L.: Correlation of conductivity and stable isotope ^{18}O for the assessment of water origin in river system, Chem. Geol., 164, 161–170, 2000.
Lee, J., Feng, X., Faiia, A. M., Posmentier, E. S., Kirchner, J. W., Osterhuber, R., and Taylor, S.: Isotopic evolution of a seasonal snowcover and its melt by isotopic exchange between liquid water and ice, Chem. Geol., 270, 126–134, doi:10.1016/j.chemgeo.2009.11.011, 2010.
Longinelli, A. and Selmo, E.: Isotopic composition of precipitation in Italy: a first overall map, J. Hydrol., 270, 75–88, 2003.
Longinelli, A., Anglesio, E., and Flora, O.: Isotopic composition of precipitation in Northern Italy: reverse effect of anomalous climatic events, J. Hydrol., 329, 471–476, doi:10.1016/j.jhydrol.2006.03.002, 2006.
Longinelli, A., Stenni, B., and Genoni, L.: A stable isotope study of the Garda Lake, northern Italy: its hydrological balance, J. Hydrol., 360, 103–116, doi:10.1016/j.jhydrol.2008.07.020, 2008.
Machavaram, M. and Whittemore, D.: Precipitation induced stream flow: an event based chemical and isotopic study of a small stream in the Great Plains region of the USA, J. Hydrol., 330, 470–480, doi:10.1016/j.jhydrol.2006.04.004, 2006.

HESSD
11, 4879–4924, 2014

Mair, E., Bertoldi, G., Leitinger, G., Della Chiesa, S., Niedrist, G., and Tappeiner, U.: ESOLIP – estimate of solid and liquid precipitation at sub-daily time resolution by combining snow height and rain gauge measurements, Hydrol. Earth Syst. Sci. Discuss., 10, 8683–8714, doi:10.5194/hessd-10-8683-2013, 2013.

Maurya, A. S., Shah, M., Deshpande, R. D., Bhardwaj, R. M., Prasad, A., and Gupta, S. K.: Hydrograph separation and precipitation source identification using stable water isotopes and conductivity: river Ganga at Himalayan foothills, Hydrol. Process., 25, 1521–1530, doi:10.1002/hyp.7912, 2011.

Meriano, M., Howard, K. W. F., and Eyles, N.: The role of midsummer urban aquifer recharge in stormflow generation using isotopic and chemical hydrograph separation techniques, J. Hydrol., 396, 82–93, doi:10.1016/j.jhydrol.2010.10.041, 2011.

Milner, A., Brown, L., and Hannah, D.: Hydroecological response of river systems to shrinking glaciers, Hydrol. Process., 77, 62–77, doi:10.1002/hyp.7197, 2009.

Molini, A., Katul, G. G., and Porporato, A.: Maximum discharge from snowmelt in a changing climate, Geophys. Res. Lett., 38, 1–5, doi:10.1029/2010GL046477, 2011.

Neal, C., Reynolds, B., Kirchner, J. W., Rowland, P., Norris, D., Sleep, D., Lawlor, A., Woods, C., Thacker, S., Guyatt, H., Vincent, C., Lehto, K., Grant, S., Williams, J., Neal, M., Wickham, H., Harman, S., and Armstrong, L.: Highfrequency precipitation and stream water quality time series from Plynlimon, Wales: an openly accessible data resource spanning the periodic table, Hydrol. Process., 27, 2531–2539, doi:10.1002/hyp.9814, 2013.

Notarnicola, C., Duguay, M., Moelg, N., Schellenberger, T., Tetzlaff, A., Monsorno, R., Costa, A., Steurer, C., and Zebisch, M.: Snow cover maps from MODIS Images at 250 m resolution, Part 1: Algorithm description, Remote Sensing, 5, 110–126, 2013.

Ohlanders, N., Rodriguez, M., and McPhee, J.: Stable water isotope variation in a Central Andean watershed dominated by glacier and snowmelt, Hydrol. Earth Syst. Sci., 17, 1035–1050, doi:10.5194/hess-17-1035-2013, 2013.

Pasolli, L., Notarnicola, C., Bertoldi, G., Della Chiesa, S., Niedrist, G., Bruzzone, L., Tappeiner, U., and Zebisch, M.: Soil moisture monitoring in mountain areas by using high resolution SAR images: results from a feasibility study, Eur. J. Soil Sci., in press, 2014.

Pearce, A. J., Stewart, M. K., and Sklash, M. G.: Storm runoff generation in humid headwater catchments, 1, where does the water come from?, Water Resour. Res., 22, 1263–1271, 1986.

HESSD
11, 4879–4924, 2014

Pellerin, B. and Wollheim, W.: The application of electrical conductivity as a tracer for hydrograph separation in urban catchments, Hydrol. Process., 22, 1810–1818, doi:10.1002/hyp, 2008.
Peng, H., Mayer, B., Harris, S., and Krouse, H. R.: A 10 year record of stable isotope ratios of hydrogen and oxygen in precipitation at Calgary, Alberta, Canada, Tellus B, 56, 147–159, 2004.
Penna, D., Stenni, B., Šanda, M., Wrede, S., Bogaard, T. A., Gobbi, A., Borga, M., Fischer, B. M. C., Bonazza, M., and Chárová, Z.: On the reproducibility and repeatability of laser absorption spectroscopy measurements for δ^2H and δ^{18}O isotopic analysis, Hydrol. Earth Syst. Sci., 14, 1551–1566, doi:10.5194/hess-14-1551-2010, 2010.
Penna, D., Stenni, B., Šanda, M., Wrede, S., Bogaard, T. A., Michelini, M., Fischer, B. M. C., Gobbi, A., Mantese, N., Zuecco, G., Borga, M., Bonazza, M., Sobotková, M., Čejková, B., and Wassenaar, L. I.: Technical Note: Evaluation of between-sample memory effects in the analysis of δ^2H and δ^{18}O of water samples measured by laser spectroscopes, Hydrol. Earth Syst. Sci., 16, 3925–3933, doi:10.5194/hess-16-3925-2012, 2012.
Penna, D., Mao, L., Comiti, F., Engel, M., Dell'Agnese, A., and Bertoldi, G.: Hydrological effects of glacier melt and snowmelt in a high-elevation catchment, Bodenkultur, 64, 93–98, 2013.
Poage, M. A. and Chamberlain, C. P.: Empirical relationships between elevation and the stable isotope composition of precipitation and surface waters: considerations for studies of paleoelevation change, Am. J. Sci., 301, 1–15, 2001.
Shanley, J. and Kendall, C.: Controls on old and new water contributions to stream flow at some nested catchments in Vermont, USA, Hydrol. Process., 16, 589–609, doi:10.1002/hyp.312, 2002.
Stewart, I.: Changes in snowpack and snowmelt runoff for key mountain regions, Hydrol. Process., 94, 78–94, doi:10.1002/hyp, 2009.
Taylor, S., Feng, X., Kirchner, J. W., Osterhuber, R., Klaue, B., and Renshaw, C. E.: Isotopic evolution of a seasonal snowpack and its melt, Water Resour. Res., 37, 759–769, doi:10.1029/2000WR900341, 2001.
Uhlmann, B.: Modelling runoff in a Swiss glacierized catchment – Part II: Daily discharge and glacier evolution in the Findelen basin, Int. J. Climatol., 33, 1301–1307, doi:10.1002/joc.3516, 2013.

HESSD
11, 4879–4924, 2014

Wassenaar, L. I., Athanasopoulos, P., and Hendry, M. J.: Isotope hydrology of precipitation, surface and ground waters in the Okanagan Valley, British Columbia, Canada, J. Hydrol., 411, 37–48, doi:10.1016/j.jhydrol.2011.09.032, 2011.

Windhorst, D., Waltz, T., Timbe, E., Frede, H.-G., and Breuer, L.: Impact of elevation and weather patterns on the isotopic composition of precipitation in a tropical montane rainforest, Hydrol. Earth Syst. Sci., 17, 409–419, doi:10.5194/hess-17-409-2013, 2013.

Yang, Y., Xiao, H., Wei, Y., Zhao, L., Zou, S., Yang, Q., and Yin, Z.: Hydrological processes in the different landscape zones of alpine cold regions in the wet season, combining isotopic and hydrochemical tracers, Hydrol. Process., 26, 1457–1466, doi:10.1002/hyp.8275, 2012.

Yde, J. C. and Tvis Knudsen, N.: The importance of oxygen isotope provenance in relation to solute content of bulk meltwaters at Imersuaq Glacier, West Greenland, Hydrol. Process., 18, 125–139, doi:10.1002/hyp.1317, 2004.

Zabaleta, A. and Antigüedad, I.: Streamflow response of a small forested catchment on different timescales, Hydrol. Earth Syst. Sci., 17, 211–223, doi:10.5194/hess-17-211-2013, 2013.

Zhang, Y. H., Song, X. F., and Wu, Y. Q.: Use of oxygen-18 isotope to quantify flows in the upriver and middle reaches of the Heihe River, northwestern China, Environ. Geol., 58, 645–653, doi:10.1007/s00254-008-1539-y, 2009.

HESSD
11, 4879–4924, 2014

Table 1. Main morphometric properties of the sub-catchments considered in the study area.

Sub-Catchment	Drainage area (km^2)	Glacierized area (%)[1]	Area with rock glacier (%)[2]	Elevation range (m a.s.l.)	Average slope (°)	Average aspect
S1	35.0	11.6	3.7	1809–3725	29.9	S
S2	27.4	14.9	3.2	2001–3725	31.8	S
S3-LSG	18.6	16.9	4.2	2151–3725	34.8	E
S4	15.4	20.4	4.4	2231–3725	32.3	S
S5-USG	11.2	26.1	4.9	2333–3725	30.8	S
S6	7.6	36.8	2.2	2401–3725	29.5	S
S7	7.5	37.3	2.3	2407–3725	29.5	S
S8	5.4	51.1	0.0	2415–3725	28.7	W
T1	10.2	0.0	3.6	1775–3280	31.5	S
T2-SG	17.5	0.9	0.2	2028–3316	19.7	W
T3	< 0.0	0.0	0.0	2159–2434	30.4	W
T4	1.22	0.0	0.0	2232–3296	35.0	W
T5	1.8	2.2	9.4	2416–3460	30.7	S
total	61.7	6.6	3.5	1632–3725	31.8	S

[1] after the South Tyrolean Glacier Inventory (Knoll, 2010); [2] after Boeckli et al. (2012).

HESSD
11, 4879–4924, 2014

Table 2. Number of rainfall, stream and spring samples collected during this study and elevation of each sampling location. RF: rainfall; S: Saldur River; T: tributaries of the Saldur River; SPR: springs. Note that samples from RF1 and RF5 were not collected in 2011. Samples from T1 were collected only in 2012, and samples from T3 only in 2011. In 2013 no tributaries were sampled and samples from the main stream were collected only at four locations (S1, S3-LSG, S5-LSG, S8). Note that S7 is the confluence just downstream S8 and T5 but after a large flood event occurred on 4 September 2011 that modified the morphology of the upper part of the Saldur River, it was moved to S6.

Sampling location	Elevation (m a.s.l.)	Number of samples
RF1	1575	12
RF2	1829	16
RF3	2154	15
RF4	2336	15
RF5	2575	8
S1	1809	66
S2	2001	32
S3-LSG	2150	89
S4	2231	20
S5-USG	2333	27
S6	2401	8
S7	2410	9
S8	2415	23
T1	1775	13
T2-SG	2027	32
T3	2159	18
T4	2242	21
T5	2415	18
SPR1	2360	15
SPR2	2348	16
SPR3	2342	16
SPR4	2334	25

HESSD
11, 4879–4924, 2014

Table 3. Parameters of the linear relationship between $\delta^{18}O$ and $\delta^{2}H$ for snow, snowmelt and ice melt samples presented in Fig. 4.

	n	slope	intercept	R^2
Snowmelt (from spring and summer snow patches)	23	8.1	9.7	0.99
Snowmelt (from snowmelt samplers)	10	7.9	4.7	0.99
Ice melt (rivulets on the glacier surface)	16	7.7	7.8	0.98
Ice melt (melting debris-covered ice)	9	7.6	5.4	0.92
Winter snowpack	22	8.2	15.0	0.97

HESSD
11, 4879–4924, 2014

Table 4. Parameters of the linear relationship between $\delta^{18}O$ and $\delta^{2}H$ for all stream water (Saldur and tributaries) and groundwater samples.

	n	slope	intercept	R^2
Stream water (Saldur River)	274	7.9	9.5	0.92
Stream water (tributaries)	102	6.5	−10.5	0.92
Groundwater	72	7.2	−1.9	0.95

HESSD
11, 4879–4924, 2014

Table 5. Average (three years) snowmelt contribution to groundwater recharge based on δ^2H data. The ± uncertainty at 70 % computed according to Genereux (1998) is reported after each estimate.

	Snowmelt contribution (%)
SPR1	71 ± 16
SPR2	72 ± 15
SPR3	70 ± 16
SPR4	58 ± 15

HESSD
11, 4879–4924, 2014

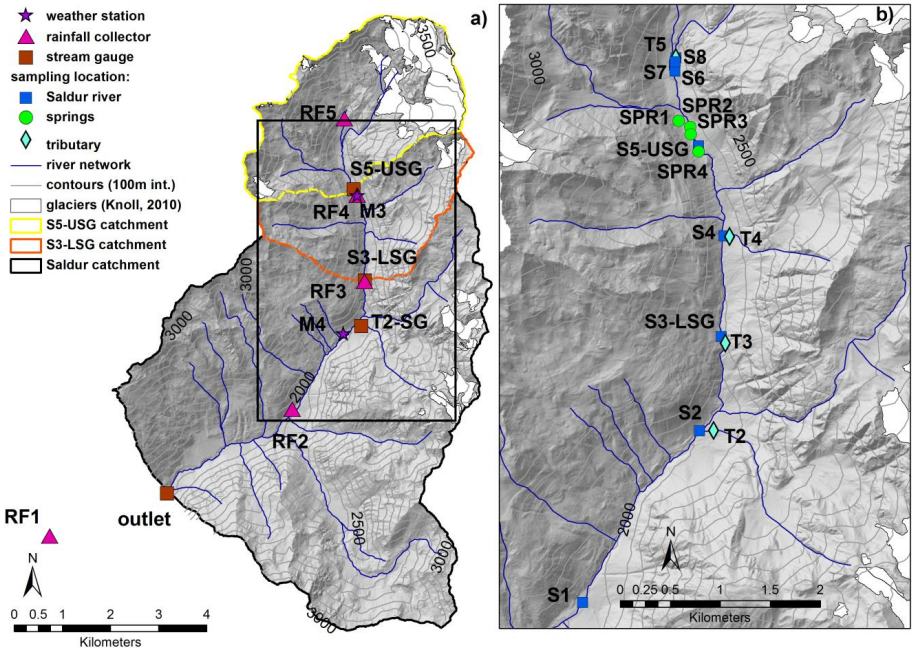

Fig. 1. Map of the Saldur catchment with position of the rainfall collectors, stream gauges and weather stations **(a)**; zoom in showing the sampling locations for isotopic and EC analysis **(b)**.

HESSD
11, 4879–4924, 2014

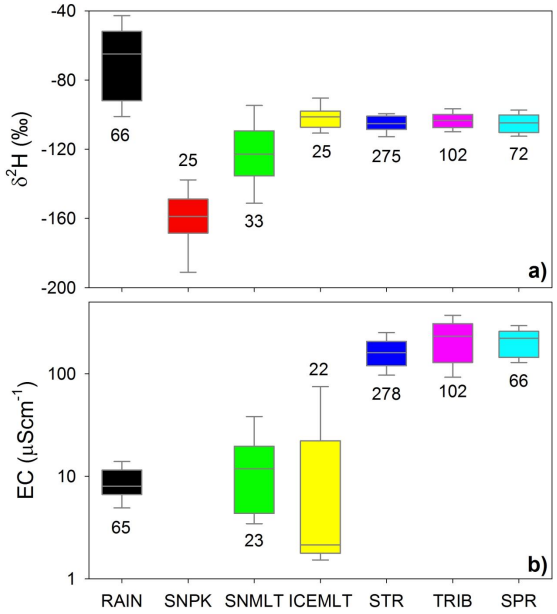

Fig. 2. Box-plot for δ^2H **(a)** and EC **(b)** of all water samples collected in this study. The whiskers represent the 10th and 90th percentiles, the box limits indicate the 25th and 75th percentiles and the line within the box marks the median. Legend: RAIN: rainfall; SNPK: winter snowpack and three samples of fresh snowfall; SNMLT: snowmelt (from patches of old snow and from snowmelt samplers); ICEMLT: ice melt (glacier melt and debris-covered ice); STR: main stream; TRIB: tributaries; SPR: springs. The numbers below or above each box represents the number of samples. EC data of the snowpack were not available.

HESSD
11, 4879–4924, 2014

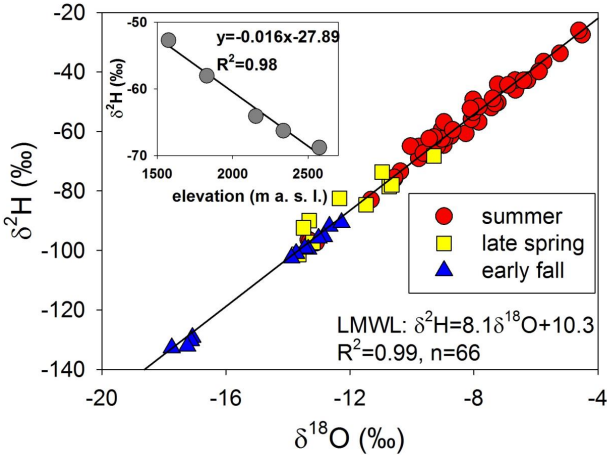

Fig. 3. Relationship between $\delta^{18}O$ and $\delta^{2}H$ values of rainfall samples collected during the monitoring period in the Saldur catchment. In the inset: average ($n = 8$) $\delta^{2}H$ in precipitation data as a function of elevation of the bulk rainfall collectors. For the inset plot, only data available for all five locations were averaged. Both correlations are statistically significant at 0.01 level.

HESSD
11, 4879–4924, 2014

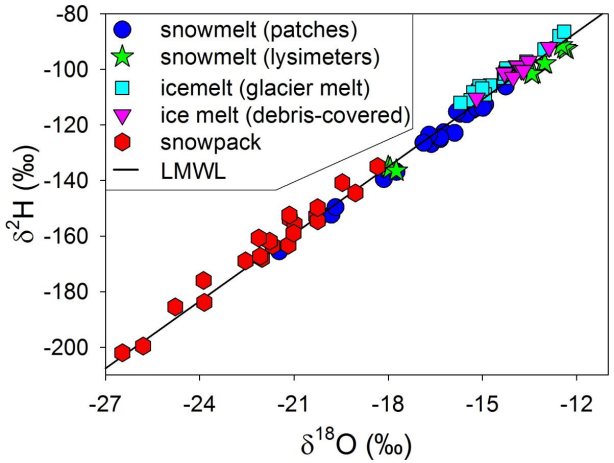

Fig. 4. Relationship between δ^2H and δ^{18}O values of snowmelt, ice melt and snow collected during the monitoring periods in the Saldur catchment.

HESSD
11, 4879–4924, 2014

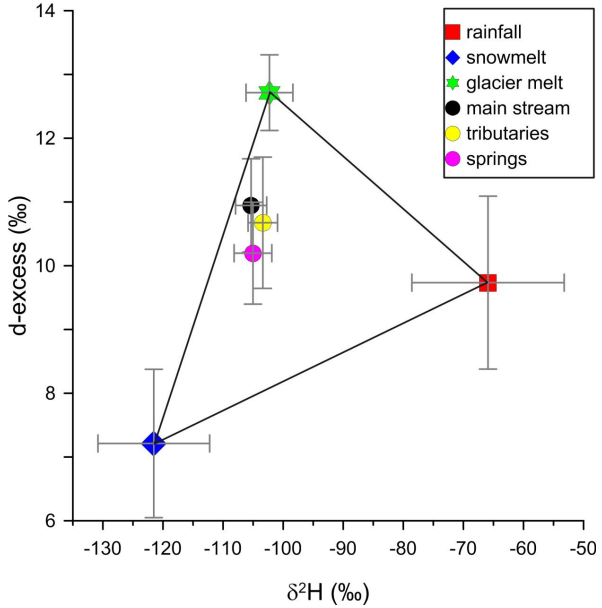

Fig. 5. Mixing diagram between δ^2H and d-excess including all average values of samples collected from the main stream, the tributaries and the springs. The error bars represent half of the standard deviation. Please note that the δ^2H and d-excess composition of rainwater samples was volume-weighted whereas this was not possible for snowmelt and glacier melt samples.

HESSD
11, 4879–4924, 2014

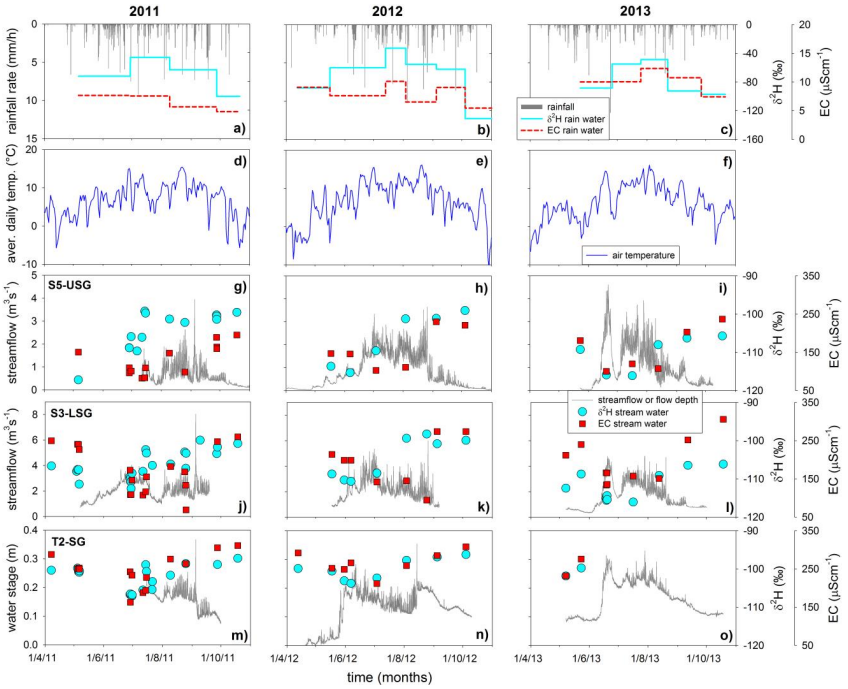

Fig. 6. Top row **(a–c)**: hourly time series of precipitation (average of values from M3 and M4), and δ^2H and EC in bulk precipitation (average of values from RF2, RF3 and RF4). Second row **(d–f)**: daily average temperature (average of values from M3 and M4). Middle row **(g–i)**: hourly time series of streamflow at S5-USG, and δ^2H and EC of stream water. Fourth row **(j–l)**: hourly time series of streamflow at S3-LSG, and δ^2H and EC of stream water. Bottom row **(m–o)**: hourly time series of water height at T2-SG, and δ^2H and EC of stream water. At S3-LSG, on five occasions in 2011, multiple samples during the day were taken but, for the sake of clarity, only three samples collected at early morning (if available), approximately at peak flow and before sunset are shown. All panels refer to the period between 1 April and 31 October, when the majority of water samples was collected.

HESSD
11, 4879–4924, 2014

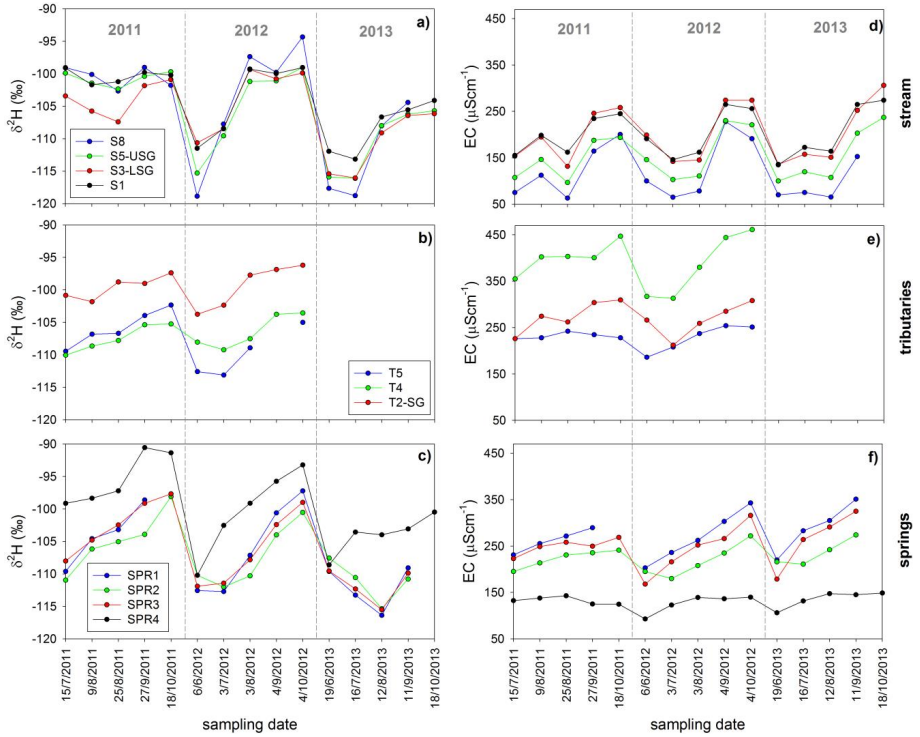

Fig. 7. Inter-annual variability of isotopic composition and EC of stream water and groundwater for the four locations in the Saldur River for which data were available for all three monitoring years **(a)** and **(d)**, the three tributaries for which the most numerous measurements were available **(b)** and **(e)** and the four springs **(c)** and **(f)** for sampling days in 2011, 2013 and 2013. Note that the spacing on the *x* axis is not proportional to the temporal distance between the sampling dates.

HESSD
11, 4879–4924, 2014

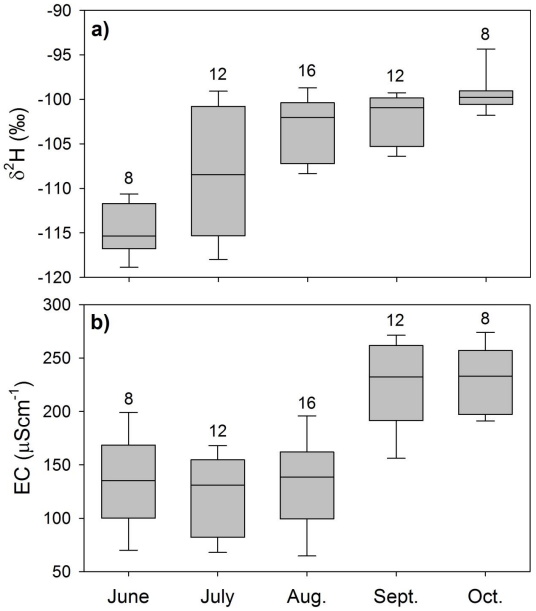

Fig. 8. Boxplot of δ^2H **(a)** and EC **(b)** of stream water data collected at the same time at the four selected locations along the Saldur River (S1, S3-LSG, S5 and S8) in 2011, 2012 and 2013 and grouped according to the sampling month. The whiskers represent the 10th and 90th percentiles, the box limits indicate the 25th and 75th percentiles and the line within the box marks the median.

HESSD
11, 4879–4924, 2014

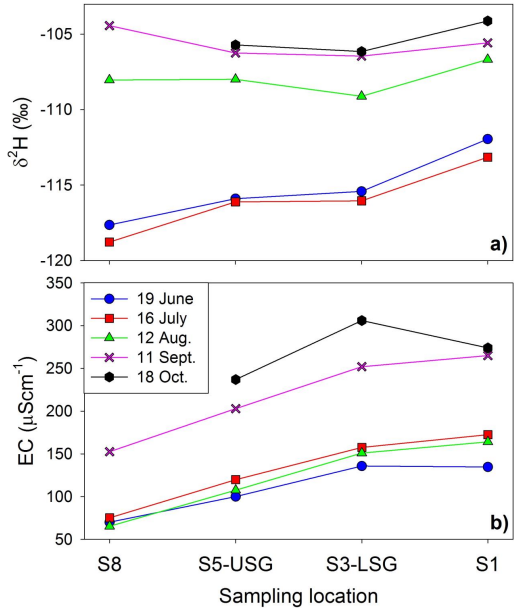

Fig. 9. Isotopic composition and EC of stream water of selected locations along the Saldur River for different sampling days during the 2013 monitoring year. Sampling started at 15:00 (UTC + 1) at S8 and ended approximately at 17:30 (UTC + 1) at S1. On 18 October it was not possible to sample location S8, sampling started at S5-USG and was carried out between 13:45 and 14:45 LT (UTC + 1).

HESSD
11, 4879–4924, 2014